ARTICLE

Single-Step Synthesis and Structural Study of Mesoporous Sulfated Titania Nanopowder by a Controlled Hydrolysis Process

K. Joseph Antony Raj and B. Viswanathan*

National Centre for Catalysis Research, Indian Institute of Technology-Madras, Chennai 600036, India

ABSTRACT An environmentally benign route for the single-step synthesis of mesoporous sulfated titania is described by a seeding method using titanium oxysulfate as the titania source. The hydrolysis was performed in the presence of NaOH and seed under constant-volume conditions around 98 °C. The XPS and DRIFT spectra show the existence of a bridged bidentate sulfate complex on the surface of titania. The elimination of sulfur on heat treatment showed a characteristic change in mesoporosity, specific surface area, and crystallinity of the material. The transformation of sulfated titania to anatase was incomplete at 900 °C, showing a delay in crystallization due to the presence of sulfur. Studies on the thermal stability of the sulfated titania showed that the material obtained can be used for various applications at temperatures below 300 °C. The ammonia-TPD and catalytic performance studies of the sulfated titania samples showed the presence of strong acid sites.

KEYWORDS: mesoporous sulfated titania • single-step synthesis • titanium oxysulfate • seeding method

INTRODUCTION

Sulfate-promoted metal oxides such as SO_4^{2-}/ZrO_2, SO_4^{2-}/TiO_2, and SO_4^{2-}/Fe_2O_3 have been developed and used as catalysts for various acid-catalyzed reactions, such as the skeletal isomerization of butane, the acylation of benzene derivatives by acyl chlorides, and the ring-opening isomerization of cyclopropane (1, 2). The sulfate ion can be introduced from H_2SO_4, $(NH_4)_2SO_4$, SO_2, SO_3, and H_2S. It was reported that the existence of covalent S−O bonds in sulfur complexes formed on metal oxides are responsible for the generation of acidity (3−5). The substitution of oxygen atoms in the titania lattice with sulfur and other anionic species (6) are reported to show photocatalytic activity enhancement in the visible range (7, 8) due to the existence of oxygen vacancies, greater surface area (9−13), and larger fraction of the anatase phase. Ohno et al. (14) reported the incorporation of sulfur in titania by sol−gel precipitation using titanium isopropoxide and thiourea and showed the enhancement in photocatalytic degradation of 2-propanol and partial oxidation of adamantane at wavelengths longer than 440 nm. Sulfated metal oxides are strong acid catalysts (15, 16) and have been classified as superacids (17). Arata (18) synthesized sulfated titania by exposing $Ti(OH)_4$ to aqueous sulfuric acid followed by calcination. Ohno et al. (14) studied the hydroxylation of adamantane using sulfated titania as catalyst, a reaction of relevance (green process) using molecular oxygen. It is reported that the activity of sulfated titania could be improved by optimizing the surface area of the sample. In general, it is conceived that Brønsted and Lewis acidity are improved by modifying TiO_2 with H_2SO_4. The acid strengths of sulfated titania catalysts have been studied (19, 20). The superacid properties of sulfated titania were considered to be responsible for the high catalytic activity in various acid-catalyzed reactions such as the alkylation of derivatives of benzene, cracking of paraffins, and dimerization of ethylene (21−25). The increase in activity for CFC-12 decomposition obtained with sulfated titania was due to the superacid properties of the catalysts (9, 26). Saur et al. (27) suggested the utility of sulfated titania for NO reduction and CO oxidation because of its noneffectiveness to sulfur poisoning. The available reports deal with a two-step preparation of sulfated titania with lower surface area and have highlighted the possible scope for improvement. The present study deals with the synthesis of mesoporous sulfated titania using titanium oxysulfate as a titania source; NaOH and a seed were employed for effecting controlled hydrolysis. The one-pot organic-free synthetic method is adopted in order to get energy savings and to meet growing environmental standards. The sulfated titania obtained by this method and its various temperature-treated samples have been characterized by BET-surface area, XRF, XRD, XPS, DRIFT spectra, TGA, nitrogen adsorption−desorption isotherm, and ammonia-TPD methods to study the effect of surface area with sulfur removal, the delaying of crystal growth by sulfates, the uniqueness of adsorbed sulfate on the surface of titania, the shift of mesoporous to nonporous titania with temperature, and the adsorption−desorption characteristics of ammonia.

EXPERIMENTAL SECTION

Chemicals. Titanium oxysulfate (Aldrich), ethanol (Hayman), acetic acid (Qualigens), and sodium hydroxide (Qualigens) were used without further purification. Double-distilled water was used as a solvent.

Preparation of Seed. Four grams of titanium oxysulfate was placed in a 100 mL SS container, and 40 mL of water was added and thoroughly mixed. The solution was heated to 70 °C with continuous stirring. Thereafter 10 wt % of sodium hydroxide was added until the pH was 2.3. The temperature of the solution

* To whom correspondence should be addressed E-mail: bvnathan@iitm.ac.in.
Received for review June 24, 2009 and accepted September 7, 2009

DOI: 10.1021/am900437u

Published on Web 10/13/2009

Table 1. Effect of BET-Surface Area on Hydrolysis Time and Temperature[a]

sample no.	temp, °C	hydrolysis time, h	BET-surface area, m^2/g	particle size, nm
1	70	12	293 ± 5.9	4.9 ± 0.1
2	80	7	289 ± 5.8	4.9 ± 0.1
3	90	5	284 ± 5.7	5.0 ± 0.1
4	98	3	275 ± 5.5	5.2 ± 0.1
5	110	2	242 ± 4.8	5.9 ± 0.1

[a] The ± sign shows the associated error of the measurements.

was maintained at 75 °C for 1 h. The obtained solution was used as a precipitation seed.

Synthesis of Sulfated Titania. A titanium oxysulfate solution containing 12% TiO_2 and 24% H_2SO_4 was employed as the starting material for the preparation of sulfated titania. To this was slowly added 10 wt % sodium hydroxide with continuous stirring until the solution was slightly turbid and the pH was 1.4. A seed solution of 5 mL was added to 83 g of titanium oxysulfate. The hydrolysis was performed in a constant boiling apparatus around 98 °C for 3 h. At the end of 3 h, the contents were rapidly transferred to a beaker containing 800 mL of water for precipitating the TiO_2 completely. The TiO_2 in hydrated form was obtained after thoroughly washing the precipitate to remove the sodium sulfate and free sulfuric acid. The precipitate obtained was dried at 100 °C for 12 h to produce sulfated titania (ST). The ST was subsequently calcined for 2 h at various temperatures such as 300, 500, 700, and 900 °C in air to study the effect of removal of sulfur from ST.

Characterization. Wide-angle XRD patterns for the calcined and as-synthesized materials were obtained using a Rigaku Miniflex II instrument, using Cu Kα irradiation. A Rigaku XRF-Primini spectrometer was used for the analysis of sulfur content in the sample. TG/DTA analyses were acquired using a Perkin-Elmer instrument, and the measurements were run in air with a temperature ramp of 2 °C/min between 40 and 900 °C using alumina as the reference. XPS measurements were recorded on a Omicron spectrometer operating in a fixed analyzer transmission mode using Mg Kα (1253.6 eV) excitation and equipped with two ultrahigh-vacuum chambers. The XPS measurements were recorded in the range of 0−800 eV. Photoelectron lines of the main constituent elements, O1s, Ti2p, and S2p, were recorded at 50 eV pass energy by 0.1 eV steps and a minimum 200 μs dwell time. All binding energies were referenced to the C1s peak at 284.8 eV. Quantitative analysis for the atomic concentration of the elements was performed by the CASA XPS program. The DRIFT spectra for the samples were recorded using a Bruker Tensor-27 instrument. The BET-surface area, pore volume, and nitrogen adsorption−desorption isotherms were measured on a Micromeritics ASAP-2020 instrument. The TPD of ammonia was measured on a Micromeritics Autochem-II/2920 instrument. Initially, the materials were degassed at 400 °C under a flow of He (25 mL/min), followed by ammonia adsorption at 25 °C for 15 min (10 vol % NH_3 in He). Subsequently, the system was purged with He for 15 min in order to remove the physisorbed ammonia, and thereafter NH_3 was desorbed by heating the sample at 10 °C/min to 500 °C under flowing He.

RESULTS AND DISCUSSION

The effect of time and temperature of hydrolysis on the surface area of the samples is seen from the data given in Table 1. The hydrolysis of titanium oxysulfate was performed using 5% seed solution at various temperatures. The rate of hydrolysis parallels the temperature. A temperature lower than 98 °C resulted in additional hours for completion of precipitation. However, these samples showed a marginal surface area increase of ca. 5% than for the hydrolysis performed at 98 °C. A hydrolysis temperature greater than 98 °C resulted in ca. 12% lower surface area and higher particle size due to an accelerated rate of hydrolysis. The addition of sodium hydroxide to titanium oxysulfate was found to be essential for lowering the free acid content and increasing the rate of the precipitation process. Similarly, the addition of seed is critical for effecting uniform hydrolysis and control of particle size. The addition of various quantities of sodium hydroxide during hydrolysis showed subtle changes in the sulfur content of sulfated titania (ST). The data reported in Table 1 show that a temperature of about 98 °C may be optimum for the hydrolysis of titanium oxysulfate.

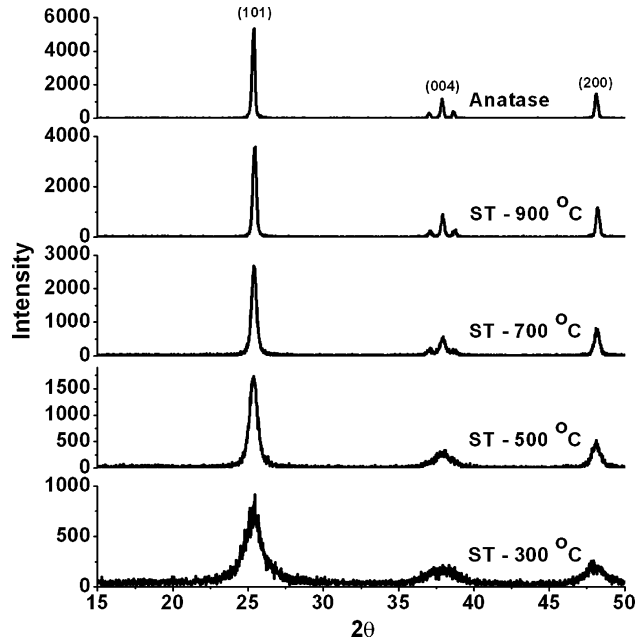

FIGURE 1. XRD patterns of sulfated titania samples calcined at various temperatures.

The XRD patterns of the anatase (Fluka) and ST samples calcined at various temperatures are shown in Figure 1. The XRD patterns showed the presence of an anatase phase in the ST samples, irrespective of the calcination temperature. In addition, the XRD data revealed that the modification of titania by polyvalent sulfate resulted in anatase type titania with the preferential reflections (101) and (004). The ST samples calcined at temperatures between 300 and 900 °C for 2 h showed increasing crystallinity with temperature. The crystallinity for calcined ST samples was calculated using a standard crystalline anatase obtained from Fluka. The ST samples calcined at various temperatures showed a crystallinity of 16−63% (Table 2). The ST calcined at 900 °C for 2 h was anticipated to produce 100% crystalline anatase. Nevertheless, the obtained crystallinity was merely 63%, which is essentially due to the sulfate content of the sample (vide infra).

Table 2 shows the pH for the 10% solution of ST samples. The pH values ranged from 2.9 to 6.9. The pH values show that prepared samples are acidic and ionic and are sus-

Table 2. Sulfur Content, Crystallinity, pH, and Proton Exchange Capacity of the Sulfated Titania Samples[a]

sample no.	sample	amt of sulfur,[b] wt %	crystallinity, %	pH of the 10% soln	proton exchange capacity, mmol/g
1	ST-100 °C	1.79 ± 0.09		2.8	1.778 ± 0.089
2	ST-300 °C	1.77 ± 0.09	16 ± 0.24	2.9	1.768 ± 0.088
3	ST-500 °C	1.04 ± 0.05	30 ± 0.45	3.3	0.902 ± 0.045
4	ST-700 °C	0.22 ± 0.01	48 ± 0.72	3.9	0.076 ± 0.004
5	ST-900 °C	nil	63 ± 0.95	6.9	nil
6	anatase	nil	100 ± 1.50	6.9	nil

[a] The ± sign shows the associated error of the measurements. [b] Sulfur content estimated by XRF.

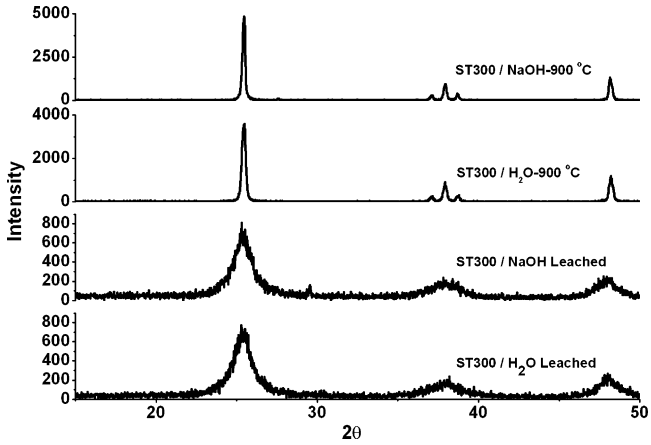

FIGURE 2. XRD patterns of sulfated titania samples leached with water and NaOH and calcined at 900 °C.

ceptible to releasing the sulfate species in the presence of water. The ST samples calcined at various temperatures showed a proton exchange capacity between 0.0758 and 1.7783 mmol/g. In order to study the leaching of sulfates from ST-300, the 10% solution of the ST-300 sample was boiled for 10 min under constant volume and thereafter titrated with 0.05 M NaOH until the pH was 7. The neutralized sample was boiled a second time for 10 min and thereafter filtered and dried at 100 °C for 12 h. The sulfur content of the ST-300 samples leached with hot water and leached after neutralizing with 0.05 M NaOH was measured by XRF, crystallinity by XRD, and weight loss properties by TGA. The sulfur content of the sample leached after neutralizing with NaOH showed 95% removal of sulfur. However, the hot water leached sample showed no more than 10% removal of sulfur, demonstrating its strong affinity with the surface of titania. The XRD patterns of the water- and NaOH-leached ST-300 and its calcined analogues (900 °C for 2 h) are presented in Figure 2. The ST-300 sample leached with water and NaOH was dried at 100 °C and measured for XRD showed same crystallinity of 15%. The samples calcined at 900 °C for 2 h and measured for XRD showed a crystallinity of 91% for the NaOH-leached sample; however, the water-leached sample showed a lower crystallinity of 67%, which is to a large extent similar to the unleached ST-300 sample. The enhanced crystallinity of 24% for the NaOH-leached sample indicates that the presence of sulfur could delay the

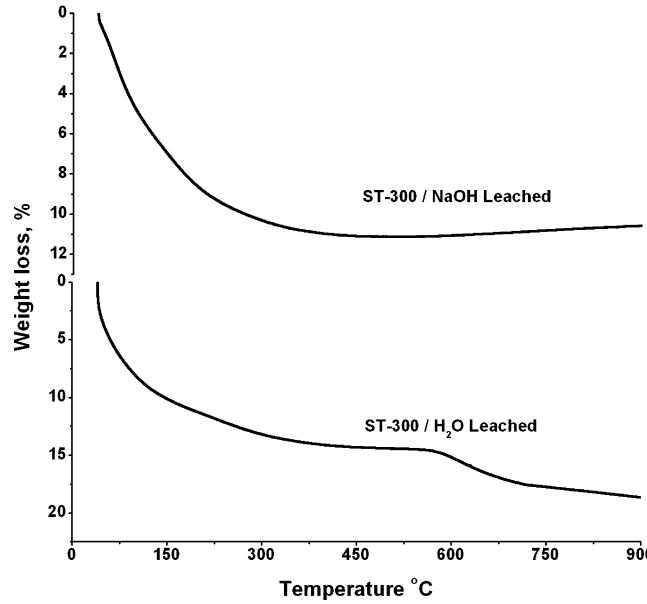

FIGURE 3. Thermograms of sulfated titania (ST-300) samples leached with H_2O and NaOH.

crystallization process. The thermograms of ST-300 samples leached with water and NaOH are shown in Figure 3. The thermogram obtained for ST-300 leached with water showed a weight loss of 13.2% up to 300 °C; this could be attributed to the removal of adsorbed hydroxyl groups and water molecules on the surface of ST-300. There was no significant weight loss observed between 300 and 550 °C. A weight loss of 3.8% was obtained between 550 and 700 °C, and this may be attributed to the removal of sulfate complexes adsorbed on the surface of ST-300. The ST-300 leached after neutralizing with NaOH showed a weight loss of 10.3% up to 300 °C, and thereafter no change in weight was observed, evidencing ca. 95% removal of sulfate species from the ST-300 sample leached with NaOH.

Table 2 shows the sulfur content of the ST samples calcined at various temperatures. The calcination of ST at 500 °C was anticipated to weaken the bond between the SO_4^{2-} and the Ti sites, which led to the removal of 41 wt % of sulfate species from ST, as shown by XRF analysis. Furthermore, the binding intensity between SO_4^{2-} and Ti(IV) in ST calcined in the range of 100−300 °C should be stronger than that of the samples calcined at higher temperatures containing lower sulfate content. The sulfate anchored to the surface of titania required greater energy for its removal, which led to nonutilization of energy for the conversion of amorphous to the anatase phase. The XRF studies showed that the surface sulfur content of the ST samples calcined at various temperatures caused a decrease in concentration of sulfur. However, the effect of sulfur removal is negligible up to 300 °C, and this shows the stability of ST during thermal treatment at less than 300 °C. It is apparent that the improved thermal stability of the ST when compared to the titania with respect to surface area and pore volume can be attributed to the formation of surface sulfur complexes (28). In general, the rutile phase formation is inevitable as the temperature is increased beyond 700 °C for the titania samples synthesized using

Table 3. BET-Surface Area, Particle Size-S_{BET} Method, Pore Volume, and Pore Size of Sulfated Titania Samples[a]

sample no.	sample	BET-surface area, m^2/g	particle size S_{BET}-method, nm	pore vol, cm^3/g	pore size, nm
1	ST-300 °C	275 ± 5.5	5 ± 0.1	0.34 ± 0.007	5.4 ± 0.11
2	ST-500 °C	101 ± 2.0	14 ± 0.28	0.29 ± 0.006	10.8 ± 0.22
3	ST-700 °C	53 ± 1.1	27 ± 0.54	0.23 ± 0.005	16.9 ± 0.34
4	ST-900 °C	21 ± 0.4	68 ± 1.36	0.15 ± 0.003	22.7 ± 0.45
5	anatase	11 ± 0.2	130 ± 2.6	0.09 ± 0.002	24.0 ± 0.48

[a] The ± sign shows the associated error of the measurements.

$TiCl_4$ and titanium isopropoxide. The adsorption of sulfate on the titania surface showed a large destabilization of the (101) surface due to the formation of a Ti−O−S linkage, resulting in a substantial decrease of the (101) fraction in the ST.

The BET-surface area, particle size, and pore volume of the ST samples calcined at various temperatures are given in Table 3. The particle size of the samples was calculated using surface area data. It is seen that there is an increase in particle size with a decrease in sulfur content of the ST and vice versa. The phase transformation of amorphous to crystalline titania of ST was found to be impeded with an increase in sulfur content, the reason being that sulfate moieties can be anticipated to break the O−Ti−O bond for the formation of a Ti−O−S linkage. In addition, the small quantity of sulfate absorbed on the titania hinders the crystal growth. The specific surface area of the ST sample was found to decrease with the calcination temperature. This is attributed to the removal of sulfate from the titania surface, which consequently results in growth of the anatase phase. In addition, the pore volume showed a trend similar to that for the surface area with temperature. The surface area, pore volume, and sulfur content data obtained for the ST samples calcined at various temperatures show that the ST may favorably be used as a catalyst for various organic transformations up to 300 °C.

XPS was employed to examine the oxidation state and the bonding characteristics of SO_4^{2-} on the TiO_2 surface. The high-resolution XPS data taken on the surface of ST calcined at 300 °C are shown in Figure 4. S/Ti ratios at the surface of ST were determined to be 0.1. The S2p XPS data are presented in Figure 4a. ST exhibited a binding energy for $S2p_{3/2}$ at 169 eV, which is associated with S−O bonds in SO_4^{2-} species (29), indicating that sulfur in the sample exists in a hexavalent oxidation state (S^{6+}). A previously established report (30) assigned the peak at a binding energy of 163−164 eV to elemental sulfur or TiS. The absence of this peak for ST reveals the absence of elemental sulfur or TiS in the sample. The binding energy of $S2p_{3/2}$ at 167.5 eV is due to SO_3^{2-} species, the absence of which in ST suggests the absence of sulfite groups in the sample. In addition, the binding energy of 169 eV matches with the $S2p_{3/2}$ data recorded for $(NH_4)_2SO_4$ (28). However, as the sulfate ions were adsorbed from an acid solution, it is less probable that the presence of the free sulfate ion in the sample explains the anchoring of sulfates on the surface of titania. The peak at a binding energy of 169 eV can be assigned to the bidentately coordinated SO_4^{2-} with the surface Ti^{4+} sites.

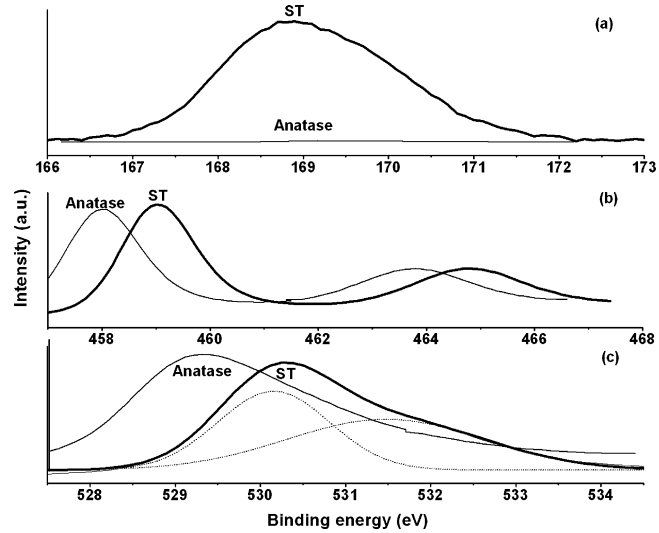

FIGURE 4. X-ray photoelectron spectra of sulfated titania calcined at 300 °C (ST-300) and anatase: (a) S 2p; (b) Ti 2p; (c) O 1s.

The XPS data for Ti 2p are presented in Figure 4b. For pure TiO_2 a binding energy of 458.1 eV was obtained for $Ti2p_{3/2}$, referenced to the C1s at 284.4 eV. The $Ti2p_{3/2}$ binding energy of the ST sample shifted to a higher value of 459.1 eV, indicating a strong interaction between the sulfate anion and titanium cation with increased positive polarity on the titanium cation. This result is consistent with the model of acid sites on solid superacids of sulfated metal oxides (11) shown in Figure 7. $Ti2p_{3/2}$ in ST can be fitted as one peak at 459.1 eV, indicating that Ti ions are in an octahedral environment, coordinated with oxygen. The XPS data for O1s are presented in Figure 4c. O1s for the anatase is composed of a single peak at 529.2 eV, corresponding to O−Ti−O in TiO_2. However, the ST sample is composed of a shoulder followed by the main peak, which is deconvoluted into a peak shown as dotted lines in Figure 4c. The O1s binding energy of the ST observed at 530.4 eV is attributed to the presence of a S−O−Ti linkage. The deconvoluted peak at a binding energy of 531.7 eV reveals the presence of two different oxygen species in the sample, and this could be due to the presence of an OH^- group, S−O bonds, or a chemisorbed water molecule. From the XPS results, the binding energies of the 2p level of Ti in ST at 459.1 eV for $Ti2p_{3/2}$ and for $Ti2p_{1/2}$ at 464.7 eV are not in accordance with the binding energies obtained for bulk TiO_2 ($Ti2p_{3/2}$ at 458.1 eV and $Ti2p_{1/2}$ at 463.8 eV), suggesting the substitution of sulfate for oxygen in the titania lattice.

Figure 5 shows the adsorption−desorption isotherm for the ST samples calcined at various temperatures. The adsorption isotherm is classified as type IV with an H4 hyster-

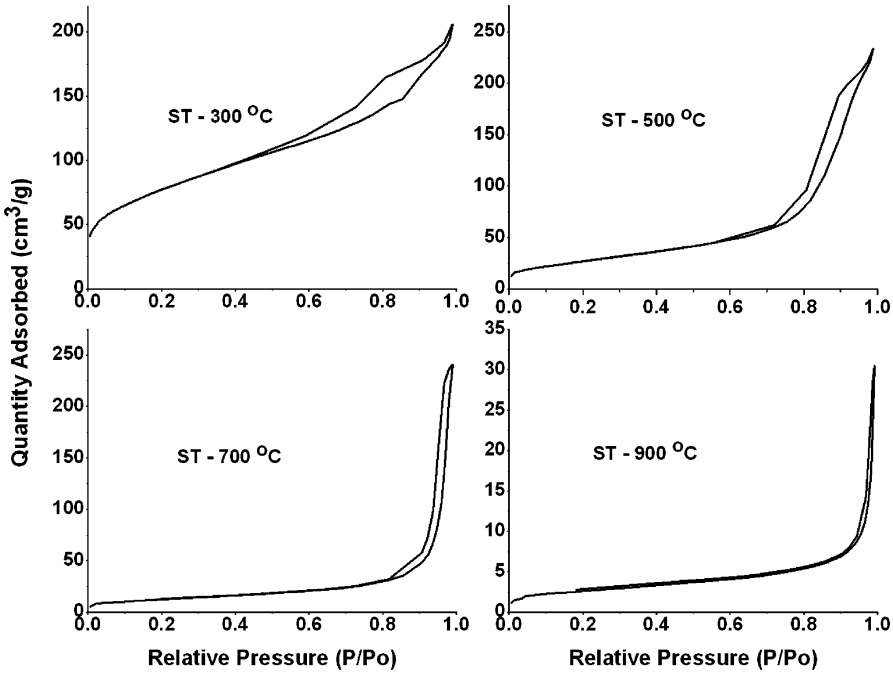

FIGURE 5. Adsorption−desorption isotherm for the sulfated titania (ST) calcined at various temperatures.

esis loop for the ST samples calcined at 300 and 500 °C. The ST calcined at 300 °C showed a steep adsorption−desorption up to 0.45 relative pressure region. Although the adsorption−desorption isotherm for ST calcined at 500 °C showed type IV with an H4 hysteresis loop, its transition to nonporous is visually evident by the isotherms calcined at 700 and 300 °C. Although ST calcined at 700 °C showed a surface area of 53 m^2/g and separate lines for adorption and desorption, the type II isotherm classified its grouping to nonporous material. The adsorption−desorption isotherm obtained for the ST calcined at 900 °C showed the same lines for adsorption and desorption explains its nonporous characteristics with type II isotherm. Hence, it is shown by the adsorption−desorption isotherms that an increase of calcination temperature from 300 to 900 °C shifted the material characteristics from mesoporous to nonporous. The decrease in pore volume and increase of particle size and pore size in the ST samples (Table 3) with an increase of temperature is attributed to the aggregation of particles and the nonexistence of small pores, which is furthermore shown by the adsorption−desorption curves given in Figure 5. A steep adsorption−desorption in the 0.4−0.6 relative pressure region is generally attributed to small pores. The ST samples calcined at 300 and 500 °C showed higher sulfur content and higher hysteresis effect in the 0.4−0.6 relative pressure region, which is characteristic of a small-pore texture with high specific surface area.

The characteristics of sulfate species on the surface of titania during calcination were examined in more detail using DRIFT spectra. A study of DRIFT spectra showed that the sulfated metal oxides which exhibited a high catalytic activity generally show a typical spectrum, which consists of a strong absorption at 1375−1390 cm^{-1} and broad bands at 900−1200 cm^{-1} (28). The DRIFT spectra for the samples were taken in the range 600−4000 cm^{-1}. Figure 6i shows the DRIFT spectra of the ST samples calcined at various temperatures; the wavelength range displayed is between 900 and 1200 cm^{-1}. A broad absorption band with five peaks is observed between 930 and 1200 cm^{-1} for the ST calcined at 300 and 500 °C. A major absorption peak was observed at 1148 cm^{-1} which is generally attributed to asymmetric stretching characteristic of sulfate vibrations (29). The other four absorption peaks were detected at about 940, 980, 1060, and 1105 cm^{-1}. If SO_4^{2-} coordinates to one or two metal ions through two of its oxygens, a chelating (Figure 7a) or a bridged (Figure 7b) bidentate complex is formed. Both complexes belong to the same point group, C_{2v}. On the basis of previous reports (4, 20, 27, 28), DRIFT spectra for the ST samples calcined at ≤500 °C showed characteristic stretching frequencies of bridged bidentate SO_4^{2-} coordinated to Ti^{4+} in the 1200−930 cm^{-1} region. This result is in agreement with the XPS data shown in Figure 4, which indicated a strong predominance of SO_4^{2-} species at the surface of ST (vide supra). The ST samples calcined at 700 and 900 °C showed a broad band of absorption without exhibiting any specific absorption in the range of 800−1200 cm^{-1} and were found to resemble crystalline anatase. Figure 6ii shows the DRIFT spectra of the ST samples displayed in the expanded range between 1200 and 1400 cm^{-1}. The range between 1200 and 1400 cm^{-1} was expanded to identify the sulfate species anchored to titania. The absorption bands appearing at 1224, 1268, 1325, and 1375 cm^{-1} for the samples calcined at 300−500 °C were due to the presence of S═O, S−O, and adsorbed water molecules in the ST sample. The band near 1375 cm^{-1} is assigned to an S═O stretching vibration; when the S═O species coordinate with water, this would appear as a S−O vibration band at a lower frequency of 1325 cm^{-1}. These bands also correspond to $(TiO)_3$−S═O and $(TiO)_2$−SO_2 asymmetric vibrations (31). It is apparent from the evaluation of XPS and DRIFT spectra

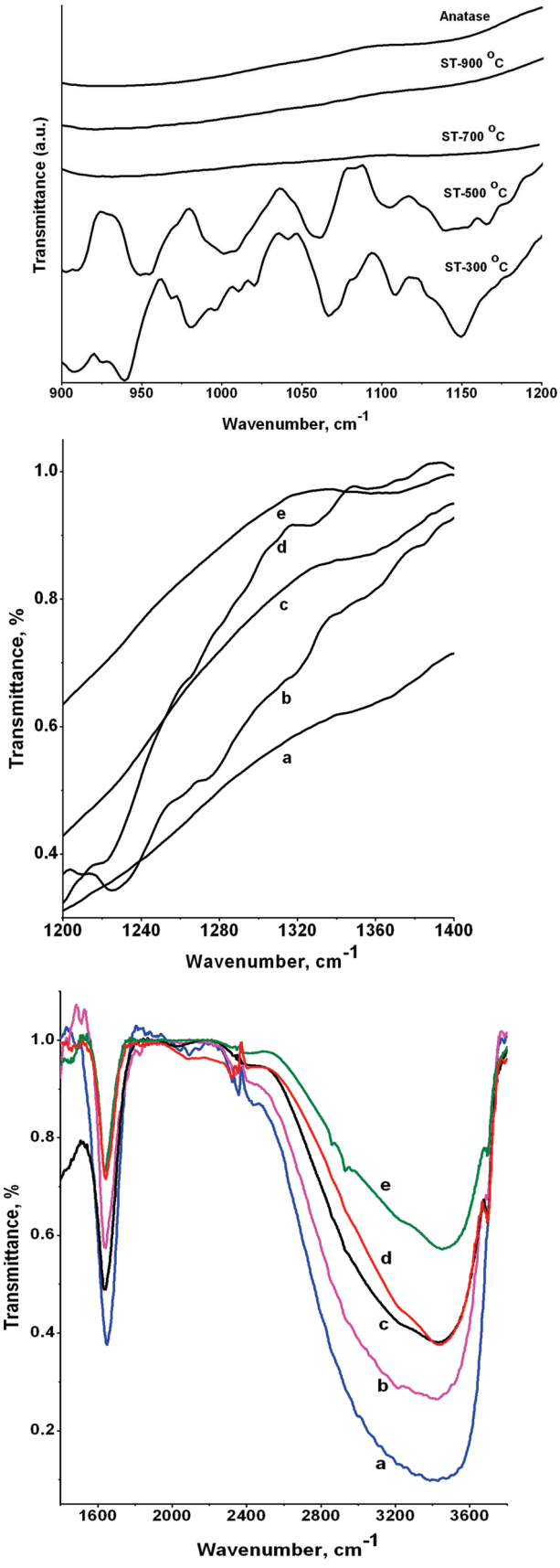

FIGURE 6. (i, top) DRIFT spectra of the sulfated titania (ST) samples calcined at various temperatures. (ii, middle) DRIFT spectra of (a) ST-700 °C, (b) ST-500 °C, (c) ST-900 °C, (d) ST-300 °C, and (e) anatase. (iii, bottom) DRIFT spectra of (a) ST-300 °C, (b) ST-500 °C, (c) ST-700 °C, (d) anatase, and (e) ST-900 °C.

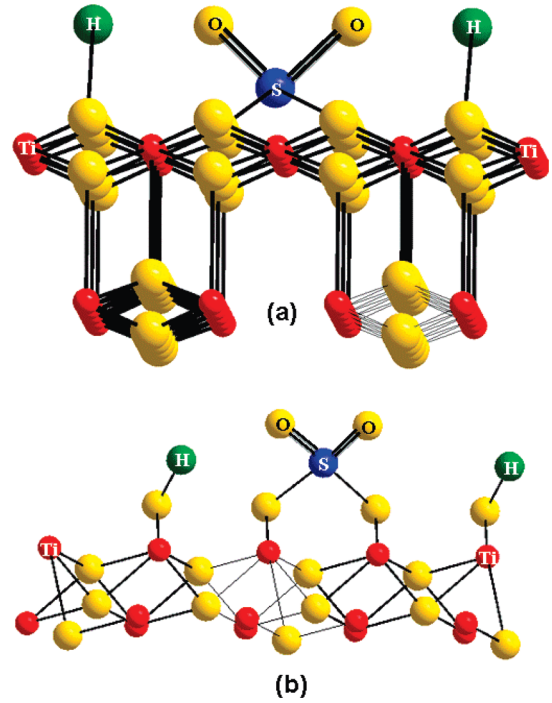

FIGURE 7. Surface structures for the sulfate formation on hydrated titania: (a) chelating bidentate; (b) bridged bidentate.

that an absorption at 1375 cm^{-1} is typical of the highest oxidation state of sulfur, S^{6+}, in S═O bonds. The ST samples calcined at 700 and 900 °C showed a single broad absorption band with low intensity at 1375 cm^{-1}, which indicated the temperature dependence of the bands appearing at 1224, 1268, and 1325 cm^{-1}. Figure 6iii shows the DRIFT spectra of the ST samples displayed in the range of 1400−3800 cm^{-1}. The sulfates at the surface of titania are thought to be mainly in the form of bidentate sulfate groups and show bands at less than 1400 cm^{-1}. The sulfates start to become polynuclear complex sulfates of possibly $S_2O_7^{2-}$ and/or $S_3O_{10}^{2-}$ type, characterized by absorptions between 1400 and 1600 cm^{-1} (32). The ST samples synthesized by the seeding method contain a maximum of 1.77% sulfur, which is equivalent to 5.3% of sulfate. Specific absorption bands were not observed between 1400 and 1600 cm^{-1} for the ST samples, indicating the absence of polynuclear sulfates. The absorption peaks at around 3400 and 1630 cm^{-1} observed in the spectra for ST samples are attributed to stretching modes of adsorbed water and hydroxyl groups. The decrease in intensity of these peaks with calcination temperature shows that they are susceptible to temperature.

The DRIFT spectra obtained for ST samples calcined at 300 and 500 °C show a number of absorption bands between 4000 and 930 cm^{-1}, which confirms the presence of ST in hydrated form and sulfates as bidentates. In the case of sulfate groups, their formation is directly linked to the degree of hydration of the material. Thus, it can be reasonably assumed that sulfate groups may be adsorbed on titania surfaces by reacting with −OH groups. In accord with the XPS, DRIFT spectra, and XRF results, sulfate formation on hydrated titania surfaces may be modeled as presented in Figure 7b.

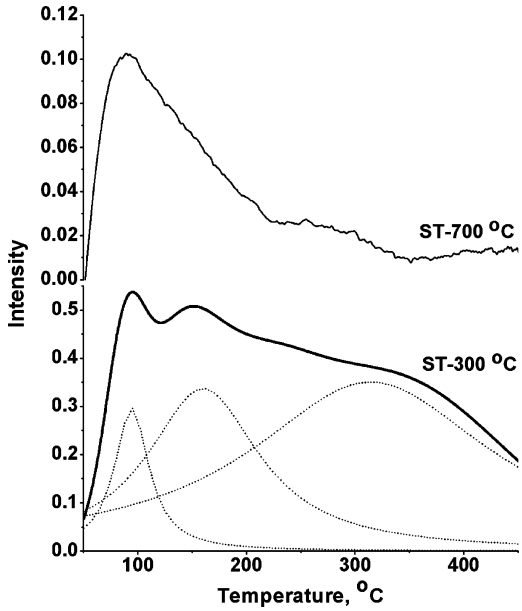

FIGURE 8. NH_3-TPD profile of sulfated titania (ST) samples calcined at 300 and 700 °C: (a) ST-300 °C; (b) ST-700 °C.

The acidity profiles obtained by ammonia-TPD for the ST samples are presented in Figure 8. ST-300 °C showed five magnitudes higher adsorption of ammonia than ST-700 °C. The TPD profile of ST-700 °C showed a peak at 100 °C and showed desorption of 80% of the ammonia at less than 235 °C. The remaining 20% of ammonia is desorbed at less than 350 °C, demonstrating the presence of weak and/or moderate acid sites on the ST-700 °C sample. The desorption profile of ST-300 °C showed peaks at 100, 168, and 320 °C and showed a desorption of 80% ammonia up to 450 °C. This explains the strong adsorption of ammonia on the surface of ST-300 °C after activation at 400 °C and demonstrates the presence of strong acid sites on ST-300 °C which is responsible for the enhanced catalytic activity.

Catalytic Activity. The esterification of acetic acid with ethanol was performed on the ST samples in a 25 mL constant-volume flask with magnetic stirring at 60 °C for 5−24 h. One gram of sulfated titania was used per 10 g of the equimolar quantity of reactant mixture. Samples were drawn periodically from the flask and analyzed for the conversion of acetic acid on a Chemito GC-1000 instrument equipped with an FFAP capillary column and FID. The reaction products were identified using GC-MS, and the GC was calibrated using pure ethyl acetate, alcohol and acetic acid mixture. The results are presented in Figure 9. The conversion of acetic acid was found to increase with contact time and showed a decreasing trend with the calcination temperature of the catalyst. The decreasing conversion is essentially due to the decreasing acidity with the elimination of sulfur from the surface of sulfated titania. ST-300 °C showed a conversion of 28%, and ST-900 °C showed a conversion of 0.9% at 24 h. Ethyl acetate was the sole reaction product obtained. The reaction was repeated with used catalyst (ST-300 °C) and showed a conversion of 26.5%, indicating that the surface deactivation is not significant for the reused catalyst. The maximum activity was

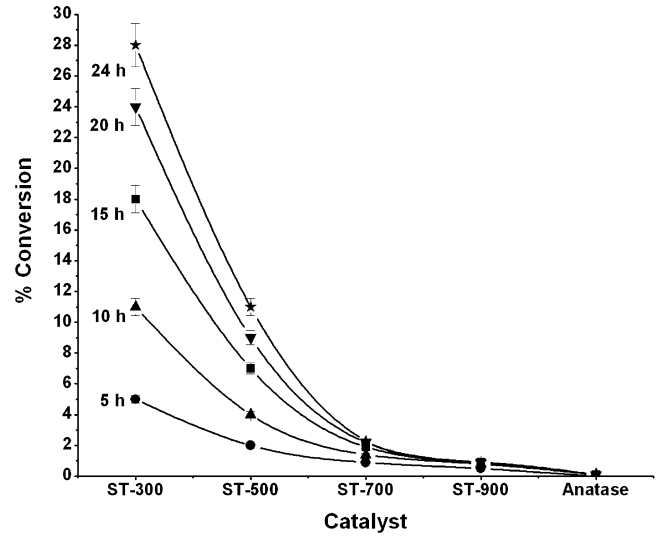

FIGURE 9. Effect of conversion of acetic acid on the various calcined sulfated titania samples.

shown over the catalyst calcined at 300 °C. The conversion of acetic acid obtained with various calcined sulfated titania shows that the reaction is not catalyzed by the titania, whereas the small quantity of sulfate remaining on the surface of titania is acting as active catalytic centers for reaction.

Generally, sulfated systems are considered as superacids. The origin and manifestation of superacidity can be associated with the multiplicity and distribution of surface sulfate species. The fact that a variety of surface species can be formed as a result of sulfatation could be a possible reason for the observation of acid sites with varying strengths, as can be seen from the results reported in this paper. The sulfate groups being hooked on as a bidentate configuration can possibly be distorted or deformed; thereby the ionicities of the bonds are considerably altered with respect to the free ions and this could be the reason for the observation of Brønsted acid sites of the reaction strength. This aspect is reflected in the results of XPS studies. Depending on the nature of the surface and the surface M−O bond characteristics, the hooked up sulfated species can manifest varying configuration and electronic properties, which could be the cause for the observation of enhanced acidity and improved catalytic activity.

CONCLUSION

The single-step synthesis of mesoporous sulfated titania has been accomplished by a seeding method. The hydrolysis of titanium oxysulfate in the presence of seed and NaOH at constant volume showed that a temperature of about 98 °C was optimum for the complete precipitation of titania. ST exhibited a high surface area of 275 m^2/g after the sample was calcined at 300 °C for 2 h. The XPS and DRIFT spectra show the formation of a bidentate sulfate complex at the surface of titania. A surface area of 54 m^2/g was obtained for the ST after calcination at 700 °C, showing the thermal stability of the material. The composition provided by XRF showed a maximum sulfur content of 1.77% for ST calcined at 300 °C.

Sulfur elimination on heat treatment in the range of 300−900 °C led to lowering of the surface area, catalytic activity, and enhancement of crystallinity. The transformation of ST to the anatase phase was only 63% when ST was calcined in air at 900 °C for 2 h, which revealed the delay in the crystallization process owing to the presence of sulfur. The acidity profile obtained by ammonia-TPD, catalytic studies, and calcination of ST at various temperatures established that the sample could favorably be used for applications at temperatures below 300 °C.

Acknowledgment. We acknowledge the Department of Science and Technology, Government of India, for funding the National Centre for Catalysis Research (NCCR) at IIT-Madras. Thanks are also due to M/s. Shell India (P) Limited for a fellowship to K.J.A.R.

REFERENCES AND NOTES

(1) Tanabe, K. In *Heterogeneous Catalysis*; Shapiro, B. L., Ed.; Texas A&M University Press: College Station, TX, 1984; p 71.
(2) Olah, G. A.; Prakash, G. K.; Sommer, J. *Super Acids*; Wiley: New York, 1985.
(3) Kayo, A.; Yamaguchi, T.; Tanabe, K. *J. Catal.* **1983**, *83*, 99–106.
(4) Yamaguchi, T.; Jin, T.; Tanabe, K. *J. Phys. Chem.* **1986**, *90*, 3148–3152.
(5) Jin, T.; Yamaguchi, T.; Tanabe, K. *J. Phys. Chem.* **1986**, *90*, 4794–4796.
(6) Asahi, R.; Morikawa, T.; Ohwaki, T.; Aoki, K.; Taga, Y. *Science* **2001**, *293*, 269–271.
(7) Zaleska, A.; Gorska, P.; Sobczak, J. W.; Hupka, J. *Appl. Catal., B* **2007**, *76*, 1–8.
(8) Ihara, T.; Miyoshi, M.; Ando, M.; Sugihara, S.; Iriyama, Y. *J. Mater. Sci.* **2001**, *36*, 4201–4207.
(9) Muggli, D. S.; Ding, L. *Appl. Catal., B* **2001**, *32*, 181–194.
(10) Su, W. Y.; Fu, X. Z.; Wei, K. M. *Acta Phys. Chim. Sinica* **2001**, *17*, 28–31.
(11) Fu, X.; Zeltner, W. A.; Yang, Q.; Anderson, M. A. *J. Catal.* **1997**, *168*, 482–490.
(12) Tanguay, J. F.; Suib, S. L.; Coughlin, R. W. *J. Catal.* **1989**, *117*, 335–347.
(13) Colon, G.; Hidalgo, M. C.; Navıo, J. A. *Appl. Catal., B* **2003**, *45*, 39–50.
(14) Ohno, T.; Akiyoshi, M.; Umebayashi, T.; Asai, K.; Mitsui, T.; Matsumura, M. *Appl. Catal., A* **2004**, *265*, 115–121.
(15) Corma, A.; Martinez, A.; Martinez, C. *Appl. Catal.* **1996**, *144*, 249–268.
(16) Lopez, T.; Bosch, P.; Tzompantzi, F.; Gomez, R.; Navarrete, J.; Lopez-Salinas, E.; Llanos, M. E. *Appl. Catal., A* **2000**, *197*, 107–117.
(17) Wan, K. T.; Khouw, C. B.; Davis, M. E. *J. Catal.* **1996**, *158*, 311–326.
(18) Arata, K. *Appl. Catal.* **1996**, *146*, 3–32.
(19) Hino, M.; Arata, K. *J. Chem. Soc., Chem. Commun.* **1979**, 1148–1149.
(20) Sohn, J. R.; Jang, H. J.; Park, M. Y.; Park, E. H.; Park, S. E. *J. Mol. Catal.* **1994**, *93*, 149–167.
(21) Hino, M.; Kobayashi, S.; Arata, K. *J. Am. Chem. Soc.* **1979**, *101*, 6439–6441.
(22) Scurrell, M. S. *Appl. Catal.* **1987**, *34*, 109–117.
(23) Hino, M.; Arata, K. *J. Chem. Soc., Chem. Commun.* **1985**, 112–113.
(24) Yori, J. C.; Luy, J. C.; Parera, J. M. *Catal. Today* **1989**, *5*, 493–502.
(25) Sohn, J. R.; Kim, H. J. *J. Catal.* **1986**, *101*, 428–433.
(26) Imamura, S.; Shiomi, T.; Ishida, S.; Utani, K.; Jindai, H. *Ind. Eng. Chem. Res.* **1990**, *29*, 1758–1761.
(27) Saur, O.; Bensitel, M.; Mohammed Saad, A. B.; Lavalley, J. C.; Tripp, C. P.; Morrow, B. A. *J. Catal.* **1986**, *99*, 104–110.
(28) Yamaguchi, T. *Appl. Catal.* **1990**, *61*, 1–25.
(29) Berger, F.; Beche, E.; Berjoan, R.; Klein, D.; Charnbaudet, A. *Appl. Surf. Sci.* **1996**, *93*, 9–16.
(30) Dutta, S. N.; Dowerah, D.; Frost, D. C. *Fuel* **1983**, *62*, 840–841.
(31) Gomeza, R.; Lopez, T.; Ortiz-Islas, E.; Navarrete, J.; Sanchez, E.; Tzompanztzi, F.; Bokhimi, X. *J. Mol. Catal. A* **2003**, *193*, 217–226.
(32) Morterra, C.; Cerrato, G.; Emanuel, C.; Bolis, V. *J. Catal.* **1993**, *142*, 349–367.

AM900437U